



# City Research Online

## City, University of London Institutional Repository

---

**Citation:** Baishya, N., Momouei, M., Budidha, K. ORCID: 0000-0002-6329-8399, Qassem, M. ORCID: 0000-0003-0730-3189, Vadgama, P. and Kyriacou, P. A. ORCID: 0000-0002-2868-485X (2020). Near infrared spectrometric investigation of lactate in a varying pH buffer. *Journal of Near Infrared Spectroscopy*, doi: 10.1177/0967033520905374

This is the accepted version of the paper.

This version of the publication may differ from the final published version.

---

**Permanent repository link:** <https://openaccess.city.ac.uk/id/eprint/24068/>

**Link to published version:** <http://dx.doi.org/10.1177/0967033520905374>

**Copyright and reuse:** City Research Online aims to make research outputs of City, University of London available to a wider audience. Copyright and Moral Rights remain with the author(s) and/or copyright holders. URLs from City Research Online may be freely distributed and linked to.

---

City Research Online:

<http://openaccess.city.ac.uk/>

[publications@city.ac.uk](mailto:publications@city.ac.uk)

---

# Near infrared spectrometric investigation of lactate in a varying pH buffer

Nystha Baishya<sup>1</sup> , Mohammad Momouei<sup>1</sup>, Karthik Budidha<sup>1</sup>, Meha Qassem<sup>1</sup>, Pankaj Vadgama<sup>2</sup> and Panicos A Kyriacou<sup>1</sup>

## Abstract

Lactic acidosis is commonly observed in various disease states in critical care and can be adopted as a hemodynamic biomarker, as well as a target for therapy. pH is the main biomarker for the diagnosis of acid-base disorders and is currently measured utilizing invasive blood sampling techniques. Therefore, there is a need for a non-invasive and continuous technology for the measurement of pH and lactate levels. In this work, near infrared spectroscopy is explored as a technique for investigating lactic acidosis. In-vitro studies on 20 isotonic phosphate buffer solutions of varying pH with constant lactate concentration (2 mmol/L) were performed. The whole near infrared spectrum (800–2600 nm) was then divided into four parts for analysis: (a) water absorption peaks, (b) 1000–1250 nm, (c) 1700–1760 nm, and (d) 2200–2400 nm. The water absorption peaks showed a linear variation with the changes in pH in the spectra. The range from 1700–1760 nm showed good correlation with calculated values for lactate ionization, with the changes in pH. However, the region from 2200–2400 nm showed a reverse correlation with respect to the concentration changes of lactate and a distinction could be made from pH 6–7 and 7–8. This study successfully identifies wavelengths (1233 nm, 1710 nm, 1750 nm, 2205 nm, 2319 nm, and 2341 nm) which can be directly correlated to lactic acidosis. Knowledge from this study will contribute toward the development of lactate-based pH monitoring optical sensor for critical care.

## Keywords

Lactate, lactic acidosis, pH, near infrared spectroscopy

## Introduction

### Background

Lactic acidosis is a form of metabolic acidosis and has been categorized into two types (Types A and B) by Cohen and Woods in 1976, depending on the presence or absence of tissue hypoxia.<sup>1</sup> Type A lactic acidosis is the more common of the two and is due to tissue hypoxia which is caused by systemic or local hypoperfusion, increased glycolytic flux, abridged oxygen-carrying capacity of the blood or reduced tissue oxygen delivery.<sup>1</sup> Type B lactic acidosis is associated with underlying disease, drugs and toxins, or with congenital disorders in metabolism. Type B can be further divided into B1, B2, and B3 which are linked with diseases such as liver failure, drugs and toxins, and innate flaws of metabolism, respectively. However, the distinction between the two types can sometimes be difficult during sepsis or septic shock as the patients manifest symptoms like circulatory dysfunction, which is typical of Type A in addition to incapacitated lactate clearance and aberrant mitochondrial function as Type B lactic acidosis.<sup>2</sup> Hence, precise estimation of lactate concentration

and pH are required in critical care to understand the underlying disease conditions.<sup>3</sup>

### pH measurements

The normal range of pH in the human body is between 7.35 and 7.45 and if the values tend toward 7.1 (severe acidemia), it has to be regulated with urgent resuscitation. Early predictions of lactic acidosis values can serve as a prognosticator for mortality in critical care.<sup>4</sup> pH in critical care is calculated using the following two equations:

*Henderson-Hasselbalch (1918).*

$$\text{pH} = 6.1 + \log \frac{[\text{HCO}_3^-]}{0.0307 \times p_{\text{CO}_2}} \quad (1)$$

<sup>1</sup>City, University of London, London, UK

<sup>2</sup>School of Engineering and Materials Science, Queen Mary University of London, London, UK

### Corresponding author:

Nystha Baishya, City, University of London, Northampton Square, London EC1V 0HB, UK.

Email: nystha.baishya@city.ac.uk

where pH is the acidity in the blood,  $[\text{HCO}_3^-]$  is the concentration of bicarbonate in the blood and  $p_{\text{CO}_2}$  is the partial pressure of carbon dioxide in the arterial blood.

*Base excess approach (1958).*

$$\text{pH} = pK + \log \frac{[\text{HCO}_3^-]}{\text{CO}_2} \quad (2)$$

Calculations are based on the Henderson–Hasselbalch equation.

$$\text{BE} = 0.02786 \times \text{PaCO}_2 \times 10^{(\text{pH}-6.1)} + 13.77 \times \text{pH} - 124.58 \quad (3)$$

While these equations are still in use for assessment of pH-dependent acid–base disorders, lactic acidosis was previously thought to occur as a result of the dissociation of lactic acid and the release of  $\text{H}^+$ .<sup>5</sup> In 2004, Robergs put forward the idea that lactate ion and not lactic acid was produced by the reaction catalyzed by lactate dehydrogenase and it consumes  $\text{H}^+$ , thus challenging the old idea that lactic acidosis was the cause of metabolic acidosis.<sup>6</sup> Stewart postulated an alternative idea of acid–base balance which could explain the role of lactic acid and was later modified by Figge and colleagues who included plasma proteins.<sup>7,8</sup> These are standards that are being followed in clinical practice and they form the basis of any arterial blood gas measurements in critical care. However, these values are based on intermittent blood sampling and can be done only at an interval of 15–20 min and hence, continuous monitoring of acid–base disorders are compromised.

The feasibility of using near infrared (NIR) spectroscopy for determination of tissue pH was first established by Soller et al. in 1996.<sup>9</sup> In their study, they considered the wavelength range from 700–1100 nm for NIR reflectance spectroscopy in skeletal muscles of rabbits. They demonstrated that NIR reflectance spectroscopy can be a feasible tool for measuring blood pH continuously. Alam et al. in 1999 showed that the wavelength range from 1500–1785 nm can be used for pH predictions in whole blood. Their study was done in an in-vitro set-up, while the prediction of pH was done incorporating multivariate techniques like partial least-squares (PLS).<sup>10</sup> The changes of pH in blood and the pertinent wavelengths which they identified were suggested to be due to histidine interaction of hemoglobin. Again, Rosen et al. considered the wavelength range from 650–1050 nm in an in-vitro reflectance NIR spectroscopy for pH prediction of whole blood using PLS models.<sup>11</sup>

All the studies mentioned above have considered reduced-range regions of the NIR spectrum for pH predictions in whole blood. These studies provide the fundamental knowledge of the feasibility of NIR

spectroscopy as a tool for estimation of blood pH. However, a detailed study is necessary to understand the inter-relationship of lactate molecule and pH in the NIR region. Hence, the motivation of this study is to understand the consequences of pH variation using the full spectral range of the NIR region (800–2600 nm) at a constant lactate concentration. This study focuses on the influence of pH on the water absorption bonds, the shape of which changes for every minute disruption in the system in accordance to the Water Mirror Approach of Aquaphotomics.<sup>12</sup> This study also focuses on the regions of the NIR spectra, where there is no influence of the water peaks; however, changes in the absorption peaks could be induced by the vibrations of the lactate molecule itself.

## Materials and methods

### Sample preparation

Twenty sample solutions of 30 mL each of varying pH (6–8), at 0.1 intervals with 2 mmol/L of lactate were prepared. A stock solution of 1 L of X1 concentration of isotonic phosphate buffer solution (PBS) was prepared in de-ionized water (Deionized Water Company, UK) with a pH of 7.4 at 24°C. The changes in pH of the stock solution (6–8) from the existing pH of 7.4 were induced by adding appropriate amounts of hydrochloric acid (HCl) or sodium hydroxide (NaOH). The range from 6–8 pH was chosen because the physiological range of pH in human body is between 7.35 and 7.45, in the absence of any pathological states.<sup>13</sup> Thereby, aliquots of the stock solution at each pH and a standard 2 mmol/L of lactate solution were used to prepare the 20 sample solutions. The pH and lactate concentration of the prepared solutions were measured using Orion Star A211 Advanced pH Benchtop Meter Kit, from Thermo Fisher Scientific, (Waltham, MA, USA) and LM5 Lactate Analyzer from Analox Instrument Limited, (Stourbridge, UK), respectively.

Na-L-lactate and isotonic PBS in dry form and HCl and NaOH (analytical grade) were purchased from Thermo Fisher Scientific (Waltham, MA, USA).

### NIR spectroscopy

Three consecutive absorbance spectra from 800–2600 nm wavelength for each sample at random were collected. A total of 60 spectra were acquired using the Lambda 1050 dual beam spectrophotometer from Perkin Elmer Corp (Waltham, MA, USA). The resolution of the spectra were maintained at step increments of 1 nm wavelength, and an average of the three spectra for each concentration was taken for analysis. A halogen–tungsten lamp was used as a light source and indium gallium arsenide (InGaAs) and polycrystalline lead sulfide (PbS) detectors were used as detectors for ranges from

800–1800 nm and 1800–2600 nm, respectively. In order to restrict oversaturation of the detectors, a Gain of 5 was introduced for the InGaAs detector, while it was kept at 1 for the PbS. The slit sizes and response times of both the detectors were kept at Servo mode and 0.2 s, respectively. Also, the reference beam was attenuated at 1% to dampen the noise at high absorbance.

The baseline correction of 100% transmittance/0% absorption was also introduced in the spectrophotometer to remove any effect of the ambient environment on the spectra; 1 mm path length quartz cuvettes (Hellma (GmbH & Co., Germany)) were used to introduce the sample in the spectrophotometer. The reference cuvette was kept blank at all times for all the samples.

### Spectral analysis

Good quality raw spectra were obtained from the spectrophotometer which were then viewed and analyzed using MATLAB R2018b, MathWorks (Natick, MA, USA). The spectral difference was done as part of pre-processing of the spectra wherein, the spectra at pH 7 was subtracted from each spectrum. The spectra corresponding to pH of 7 was considered because of the acid–base neutrality of the solutions. Further pre-processing was done using Extended Multiplicative Scattering Correction (EMSC) with quadratic polynomial baseline correction to reduce multiplicative effects.<sup>14</sup> For the Savitzky–Golay, different window sizes (7,31,51 & 71) were tried and tested. In order to counter-balance the noise enhancement effects of first order differentiation a window size of 71 was selected.<sup>15</sup> The spectral analysis was done using 2D correlation to better understand the variations on the spectra arising due to systematic changes in the pH of the solution samples.

## Results

### pH and NIR spectra

The averaged raw spectra of the 20 samples were compiled together in Figure 1. In this figure, the

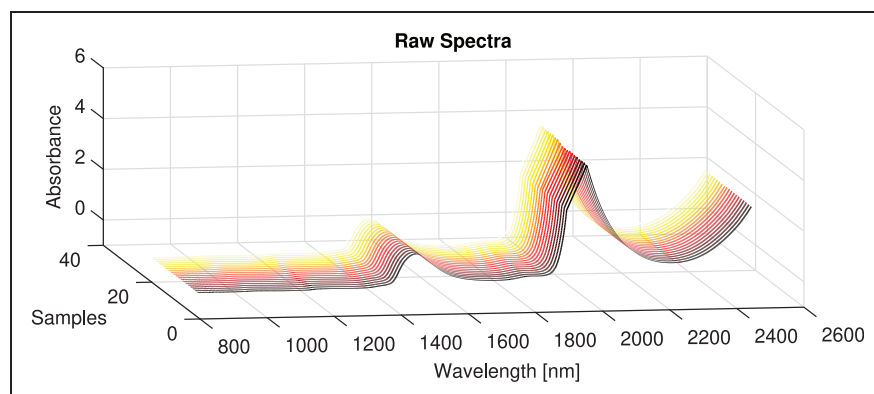


**Figure 1.** Raw NIR spectra of 20 samples with pH 6–8, at 0.1 intervals.

absorption of the first –OH stretch (1300–1600 nm) and the combination of –OH bending and stretching (1800–2200 nm) can be observed.

For better visualization of minute spectral variations, the spectra were divided into two sets; pH of 6–7 and 7–8. Visual inspection of both sets shows that with varying pH, there are definite changes in the water absorption peaks. To amplify these changes further, pre-processing (EMSC and smoothing by Savitzky–Golay) on the two sets were done separately and they are as shown in Figure 2.

### pH and lactate concentration

From basic analytical chemistry, the concentration of lactate in the prepared solution samples can be calculated from the Henderson–Hasselbalch equation

$$\text{pH} = \text{p}K_a + \log \frac{[A^-]}{[HA]} \quad (4)$$

In this equation, pH is changing from 6–8;  $\text{p}K_a$  of lactic acid is 3.8 and 2 mmol/L of standard lactate solution was added while preparing the sample solutions. The calculated (actual) lactate concentrations in the sample solutions vs pH plot are as shown in Figure 3. From this plot, we see a decreasing trend of a second-degree polynomial order in the concentrations of lactate, as the pH is increasing from 6–8. This decrease of concentration is due to the ionization of lactate from  $\text{C}_3\text{H}_6\text{O}_3$  to  $\text{C}_3\text{H}_5\text{O}_3^-$ .

### Lactate concentrations and NIR spectra

Rigorous studies done previously, for the purpose of fingerprinting the lactate molecule based on vibrational spectroscopy, shows that the peaks 1142 nm, 1233 nm, 1710 nm, 1750 nm, 2205 nm, 2319 nm, and 2341 nm correlate well with the lactate concentration changes in the NIR spectrum. Hence, the absorbance values of those peaks were identified in the spectra in Figure 2. The absorbance values vs pH for each of those wavelengths are plotted in Figure 4.

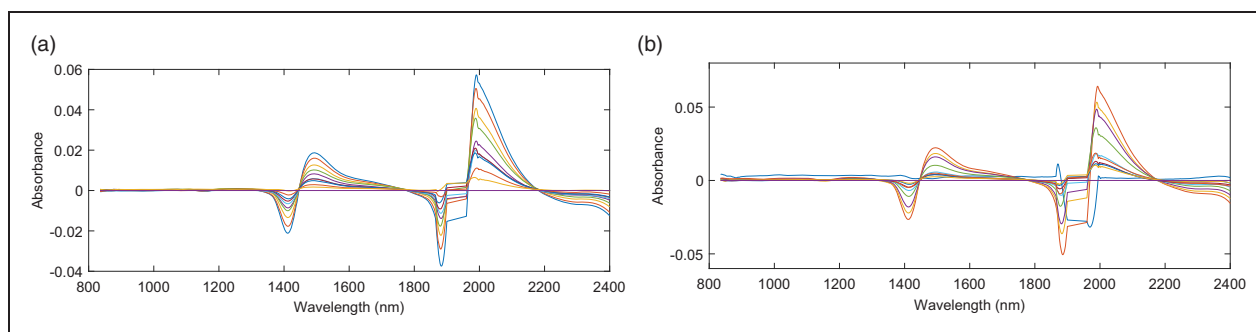


**Figure 2.** Pre-processed spectra, extended multiplicative scatter correction (EMSC) and Savitzky-Golay filtering of pH 6-8. (a) Pre-processed spectra of pH 6-7 and (b) pre-processed spectra of pH 7-8.

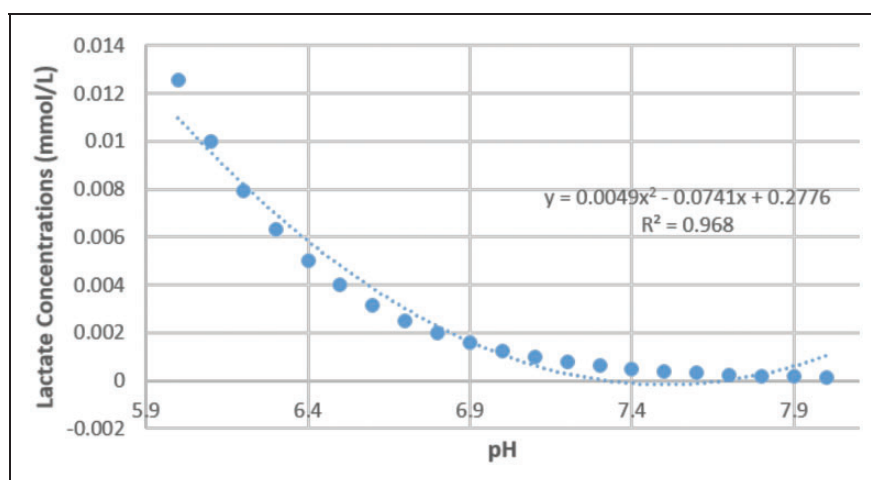


**Figure 3.** Calculated lactate concentrations vs pH.

## Discussion

### Water absorption peaks

As discussed above, the water absorption peaks at 970 nm, 1450 nm, and 1960 nm shows visible changes as the pH of the solution sample changes from 6-8. These hyperchromic shifts in the absorbance values can be associated with the changes in overtone bands of water which occur due to linear combinations of stretching and bending vibrations in the water molecule. Previous studies have been done on these regions of the NIR spectra in order to understand the contributions of water in biological systems. For example, perturbations in the spectra due to changes in temperature or protein conformations have demonstrated systematic variations in a new field of science known as Aquaphotomics.<sup>12</sup> To understand this better in regards to precise changes in pH, linear regressions on those peaks were performed, which confirms that the changes in pH can be seen as linear increase in the absorption values of these peaks, with  $p$ -values  $< 0.05$ . Table 1 shows the water absorption peaks with the corresponding  $p$ -values in the spectra.

### Lactate absorption peaks

For the rest of the wavelength range from 1000 to 2400 nm, the spectra were divided into three regions; 1000-1250 nm, 1700-1760 nm, and 2200-2400 nm, for better understanding of the absorbance. It is seen that for the first region, 1000-1250 nm, the absorbance values in wavelength 1142 nm do not follow any trend with respect to the changes in the pH (Figure 4). However, the absorbance values in wavelength 1233 nm shows a decreasing negative trend, with  $R^2 = 0.80$ . These wavelengths appear in the spectra as a result of the C-H second overtone.

For the second region, 1700-1760 nm, from Figure 4, the wavelengths 1710 nm and 1750 nm has a continuous steep decline in second-degree polynomial order in the absorbance values can be seen with increase in pH,  $R^2 = 0.91$ ,  $0.90$ , respectively. These wavelengths can be associated to the C-H stretch first overtone in the spectra.

Finally, in the region from 2200 to 2400 nm, the wavelengths 2205 nm, 2319 nm, and 2341 nm follow a second-degree polynomial order curve with  $R^2$  values of 0.96, 0.94, and 0.90, respectively, with the changes

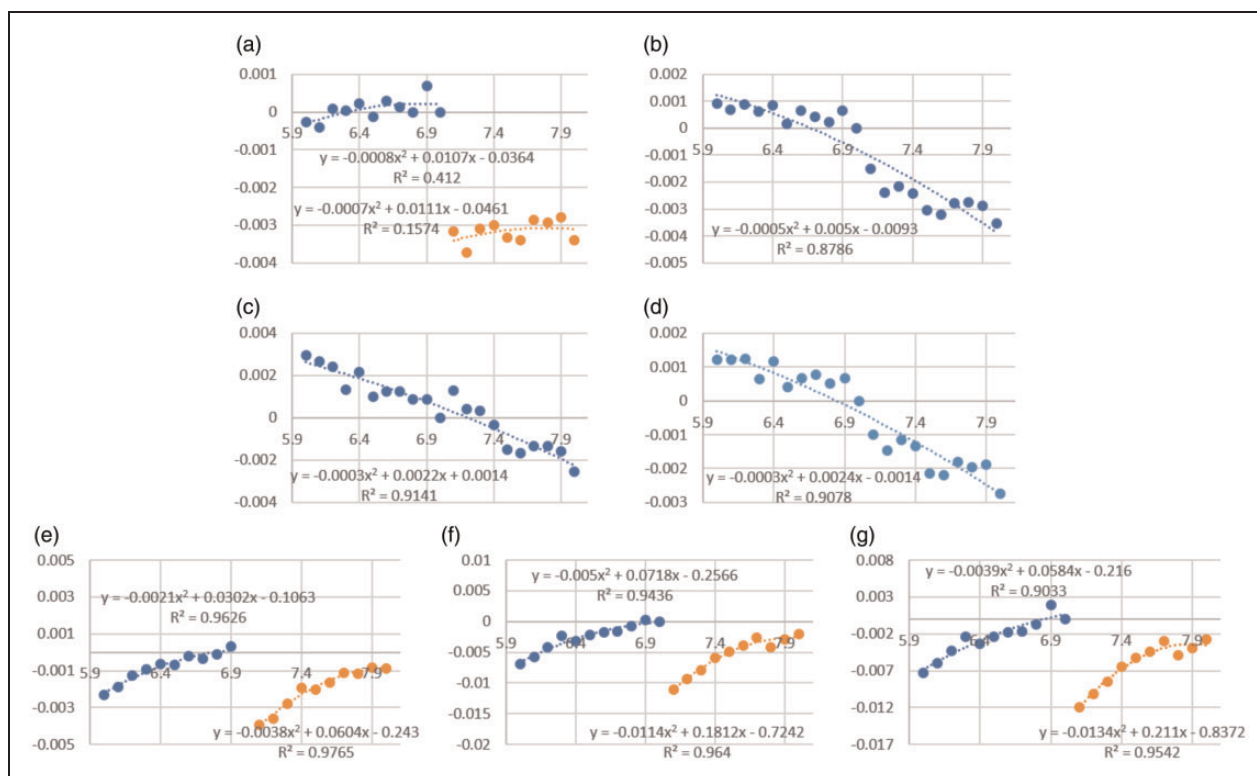


**Figure 4.** Absorbance values of monochromatic wavelengths: (a) 1142 nm, (b) 1233 nm, (c) 1710 nm, (d) 1750 nm, (e) 2205 nm, (f) 2319 nm, and (g) 2341 nm for pH 6–8.

**Table 1.** *p*-Values of the water absorption peaks in near infrared region.

Wavelengths corresponding to water molecule (nm)	Functional groups	<i>p</i> -Values
970	O–H stretch	1.8e-06
1450	O–H stretch first overtone	4.0e-09
1490	O–H stretch first overtone	0.023
1540	O–H stretch first overtone	0.0029
1820	O–H stretch	0.0758
1960	O–H stretch/O–H bend combination	2.3e-09
2070	O–H combination	0.0187
2100	O–H bend	0.0086

in pH from 6–7. There is a dip in the value from 6.9–7.1, which provides necessary confidence to evaluate the values pertinent to critical care in a more detailed manner, separately. While, the absorbance values from 7.1–8, follows another second-degree polynomial curve with  $R^2$  values of 0.97, 0.96, and 0.95, respectively, as seen in Figure 4. The wavelength 2205 nm can be associated with C–H stretch/C=O stretch combination, while the wavelengths 2319 nm and 2341 nm can be correlated to C–H bend second overtone and C–H stretch/C–H deformation, respectively.

### NIR absorption peaks and lactate concentrations

In all the monochromatic wavelengths, discussed above, the absorbance values can be observed to be fitted to a second-order polynomial. For wavelengths, 1233 nm, 1710 nm, and 1750 nm, there is a steep decline in the absorbance values, whereas, for wavelengths, 2205 nm, 2319 nm, and 2341 nm, there is a steep increase in the values. The absorbance values in a sample can always be interrelated to the concentration of the sample using the Beer–Lambert law, which states that

$$A \propto C \quad (5)$$

where,  $A$  is the absorbance of the sample solution at a particular wavelength and  $C$  is the concentration of the solution.

Hence, from Figures 3 and 4, the absorbance values at those marked wavelengths can be consociated with the concentration of calculated lactate concentrations which changes due to ionization.

Hence, from these results, it can be seen that the wavelength range 1700–1760 nm reflects the concentration changes due to ionization of lactate. However, the wavelength range 2200–2400 nm shows changes in the spectra due to changes in pH but in an upward trend. A distinct difference can be seen in the pH changes from 6–7 and 7–8. The upward trend might be due to the polarization of the L(+)-lactate

stereoisomer because lactate is optically active due to the presence of a chiral carbon. While the marked distinction between pH values of 6–6.9 and 7.1–8 (Figure 4) might be due to the complete ionization of the lactate molecule itself.

## Conclusions

For the first time, the entire NIR spectral range was considered for investigating the perturbations of the spectra due to lactic acidosis. Although NIR spectra have been used for similar predictions before, the behavior of different pH values with the same lactate concentration was not investigated. From this study, it can be seen that the monochromatic wavelengths 1233 nm, 1710 nm, 1750 nm, 2205 nm, 2319 nm, and 2341 nm reflect the changes of lactate molecule ionization with changes in pH in accordance to theoretical calculations. More precise investigations for pH changes in the clinical ranges (7.35–7.4) could provide more accuracy for prediction of pH values, when the lactate concentrations are known. Also, better understanding of the inter-relationship between lactate and pH in terms of acid–base physiology will provide more oversight in future studies. The knowledge from this study will provide a platform for further development of NIR-based optical technology for determining continuous pH levels in critical care, which will aid clinicians in the better assessment of acid–base disorders. Moreover, clinical applications demand the use of NIR spectroscopy for more complex samples like plasma/serum, whole blood over skin and tissue layers, adding to complications in spectral acquisition and analysis. These issues can be overcome using specific multi-variate models developed for this application.

## Declaration of conflicting interests

The author(s) declared no potential conflicts of interest with respect to the research, authorship, and/or publication of this article.

## Funding

The author(s) disclosed receipt of the following financial support for the research, authorship, and/or publication of this article. This research was supported by the Engineering and Physical Sciences Research Council (EPSRC) under the Healthcare Technologies theme (EP/R003750/1).

## ORCID iD

Nystha Baishya  <https://orcid.org/0000-0002-2231-6132>

## References

1. Cohen RD and Woods HF. Lactic acidosis revisited. *Diabetes* 1983; 32: 181–191.
2. Park R. Lactic acidosis. *West J Med* 1980; 133: 418–424.
3. Levy B, Desebbe O, Montemont C, et al. Increased aerobic glycolysis through beta2 stimulation is a common mechanism involved in lactate formation during shock states. *Shock* 2008; 30: 417–421.
4. Samanta S, Singh RK, Baronia AK, et al. Early pH change predicts intensive care unit mortality. *Indian J Crit Care Med* 2018; 22: 697–705.
5. Zilva JF. The origin of the acidosis in hyperlactataemia. *Ann Clin Biochem* 1978; 15: 40–43.
6. Robergs RA, Ghiasvand F and Parker D. Biochemistry of exercise-induced metabolic acidosis. *Am J Physiol Regul Integr Comp Physiol* 2004; 287: R502–R516.
7. Luchette FA, Jenkins WA, Friend LA, et al. Hypoxia is not the sole cause of lactate production during shock. *J Trauma* 2002; 52: 415–419.
8. Gunnerson KJ, Saul M, He S, et al. Lactate versus non-lactate metabolic acidosis: a retrospective outcome evaluation of critically ill patients. *Crit Care* 2006; 10: R22.
9. Soller BR, Micheels RH, Coen J, et al. Feasibility of non-invasive measurement of tissue pH using near-infrared reflectance spectroscopy. *J Clin Monit* 1996; 12: 387–395.
10. Alam MK, Rohrscheib MR, Franke JE, et al. Measurement of pH in whole blood by near-infrared spectroscopy. *Appl Spectrosc* 1999; 53: 316–324.
11. Rosen NA, Charash WE and Hirsch EF. Near-infrared spectrometric determination of blood pH. *J Surg Res* 2002; 106: 282–286.
12. Tsenkova R, Munćan J, Pollner B, et al. Essentials of aquaphotomics and its chemometrics approaches. *Front Chem* 2018; 6: 363.
13. Hopkins E and Sharma S. *Physiology, acid base balance*. StatPearls [Internet]. Treasure Island, FL: StatPearls Publishing, 2018.
14. Geladi P, MacDougall D and Martens H. Linearization and scatter-correction for near-infrared reflectance spectra of meat. *Applied spectroscopy* 1985; 39(3): 491–500.
15. Savitzky A and Golay MJ. Smoothing and differentiation of data by simplified least squares procedures. *Analytical chemistry* 1964; 36(8): 1627–1639.